



NUMERICAL THREE-DIMENSIONAL MODELLING OF THE LANDSLIDE PROCESS IN THE CARPATHIAN FLYSCH

Lesław ZABUSKI¹

Abstract. The paper presents possibility and results of numerical simulation of the landslide movement, performed for three-dimensional (3D) model. As it is commonly known, flysch rock mass has an anisotropic nature and thus exhibits different behaviour, depending on the orientation of the geologic structures with respect to the morphology of the terrain. If two-dimensional (2D) model of the slope built of such rock mass is constructed, many spatial properties are lost. On the contrary, 3D analysis allows taking into account also the spatial distribution of the structures and, in consequence, mechanical properties of the modelled rock mass.

The example of the Kawiory landslide slope analysed in the paper illustrates the modelling procedure, and the results proving the advantages of 3D approach. The computer program FLAC3D (Itasca, 1997), based on the finite difference method, was used for simulation.

Key words: finite difference method, numerical model, landslide, Carpathian flysch.

Abstrakt. W artykule omówiono możliwości oraz przedstawiono wyniki symulacji numerycznej ruchu osuwiskowego, wykonanej na przestrzennym modelu zbocza. Fliszowy masyw skalny charakteryzuje się anizotropią i — co za tym idzie — jego zachowanie zależy od orientacji struktur geologicznych w relacji do morfologii powierzchni terenu. Model dwuwymiarowy często nie pozwala na uwzględnienie takich struktur. W takich sytuacjach jedynie zastosowanie modelowania przestrzennego (3D) umożliwia stosunkowo dobre odwzorowanie przestrzennych cech ośrodka.

Przedstawiono przykład analizy przestrzennej procesu deformacji zbocza osuwiskowego Kawiory, wykazując zalety metody 3D. Symulację numeryczną procesu przeprowadzono przy użyciu programu FLAC3D (Itasca, 1997), opartym na metodzie różnic skończonych.

Słowa kluczowe: metoda różnic skończonych, model numeryczny, osuwisko, flisz karpacki.

INTRODUCTION

The Kawiory landslide represents the “mature” process, which nowadays is in very advanced deformation stage. The map prepared over 30 years ago (Fig. 1) proved that the process was distinctly marked in that time and it is still active today. The landslide is situated in Beskid Niski Mts., in the peripheral part of the

Magura Nappe. The rocks forming the slope — variegated shales — are weak and prone to water action. In the upper part, inoceramus beds are present containing thin sandstone and shale layers. A thin layer of the Quaternary deposits covers the slope surface. The inclination of the slope varies between 7 and 13°.

¹ Polish Academy of Sciences, Institute of Hydro-Engineering, Kościarska 7, 80-953 Gdańsk; e-mail: lechu@ibwpan.gda.pl

MODELLING OF THE SLOPE

The morphological 3D model using FLAC3D (Itasca, 1997) (Fig. 2) was constructed on the base of the slope map. As it could be seen, the two niches which were in the upper and the lowest parts of the slope were eroded and undercut by the Ropa River.

The geological heterogeneity as well as the position of the soil and rock mass were modelled by changing the geo-mechanical parameters of the material, both in vertical and horizontal directions. The following information taken from different sources (e.g. maps, laboratory tests of mechanical properties) constitute the base of the model:

- deformational dynamics was greatest in the lowest part of the slope;
- the movement was most active in SW–W part; the NE–E region was more stable;
- river bank was occasionally unstable, although its changes were rather slow;
- landslide activity in the middle part of the slope was differentiated: the lateral zones were the most active whereas the central part was relatively stable (see Fig. 1);
- two niches were developed in the uppermost part of the landslide.

Shear strength parameters were determined in laboratory tests (Zabuski *et al.*, 2004). Their values exhibit large dispersion; cohesion varies between 2 and 190 kPa, and friction angle varies between 2.9 and 20.6°. Finally, constant value of the friction angle was used, equal to 4°. On the contrary, cohesion of the modelled medium changed both in X and Y directions, according to the formulae:

$$c_x = c_0 - D_x \cdot (X_0 - X) \text{ in X direction;}$$

$$c_y = c_0 - D_y \cdot (Y_0 - Y) \text{ in Y direction,}$$

where: c_0 — cohesion in the central part of the slope ($c_0 = 1 \text{ kPa}$);
 $D_x = 0.065$, $D_y = 0.04$.

The resulting distribution of the slope cohesion is shown on Figure 3.

Shear strength parameters in the deeper (bedrock) zones were constant: $c = 12 \text{ kPa}$, $\phi = 15^\circ$. Values of other parameters are listed below:

- elasticity modulus $E = 100 \text{ MPa}$,
- poisson's coefficient $\nu = 0.35$,
- dilatation angle $\psi = 0.25$,
- uniaxial tension strength $\sigma_t = 0$.

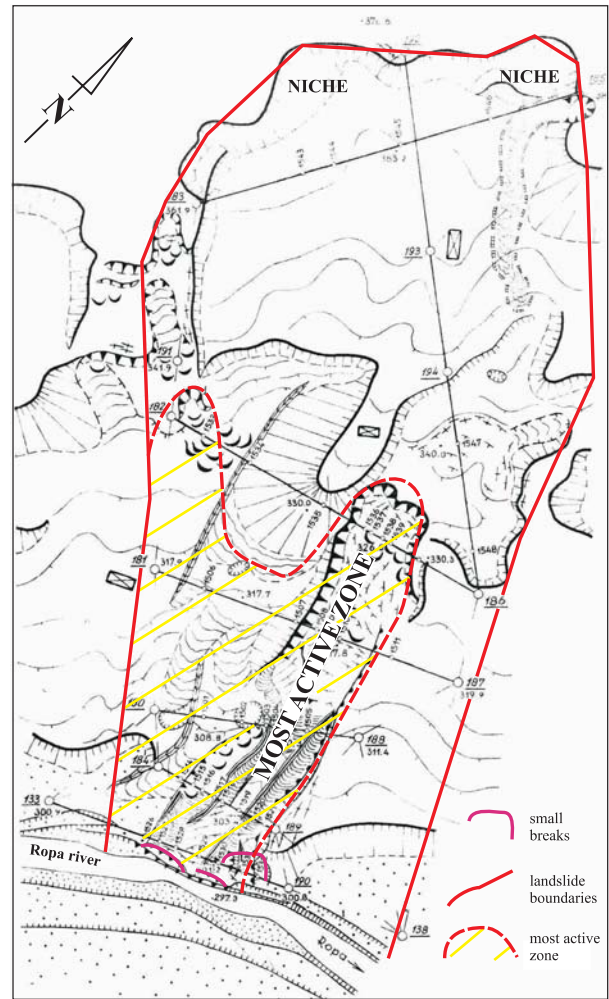


Fig. 1. Map of the Kawiory landslide with signed lines of the horizontal displacement measurements (after Dauksza, Kotarba, 1973)

Water presence was modelled in the form of the continuous groundwater table.

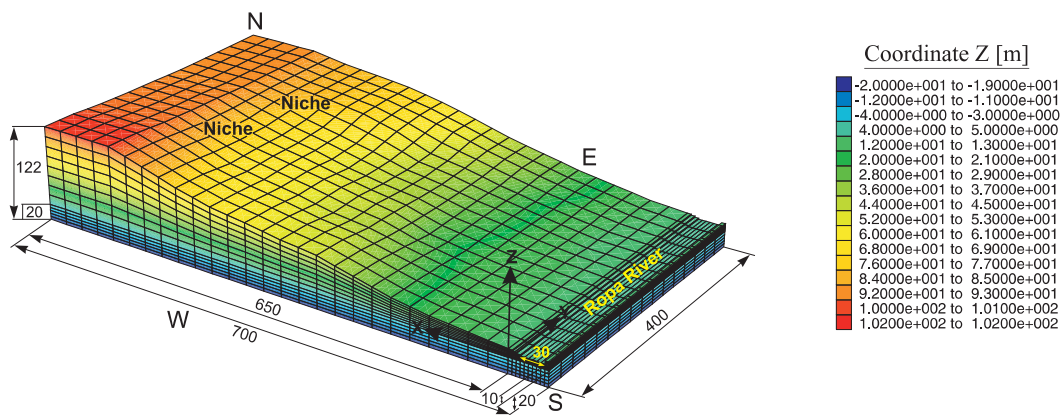


Fig. 2. Spatial model of the Kawiory landslide slope

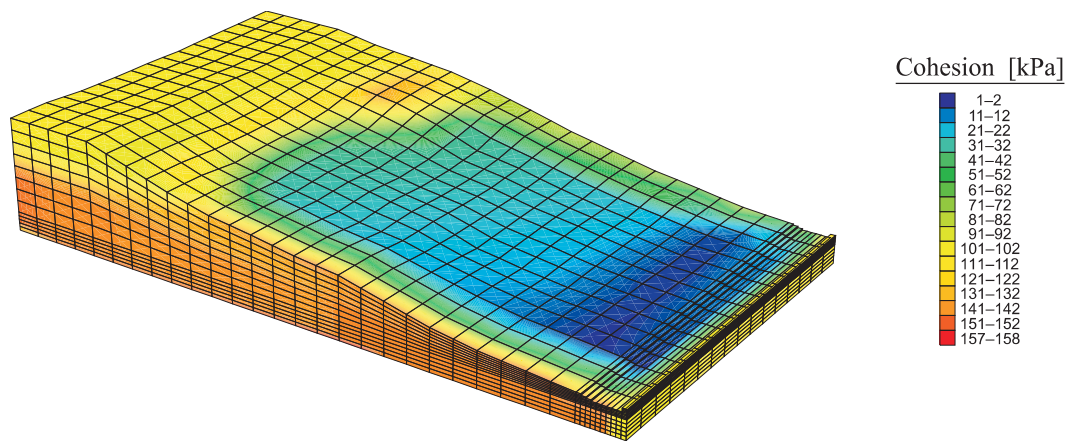


Fig. 3. Distribution of the material cohesion in the slope

RESULTS OF NUMERICAL SIMULATION

The results of calculation in form of the X, Y and Z displacement components are presented on Figure 4. It is clear that the displacements occur not only in X–Z plane; a component occurs also in Y direction, which is equal to few metres. This component would not be registered in case of two-dimensional calculations. It proves the advantage of 3D approach.

Moreover, it is possible to observe a differentiated landslide shape, especially changing the slide surface depth in different longitudinal sections. Figure 5 presents the distribution of the shear strain increments SSI in the two selected sections of the landslide. This quantity allows finding the regions with the most active deformation velocities. The greater was SSI, the more intensive was the movement. The SSI values in $Y = 75\text{--}100$ m section are greater than in $Y = 375\text{--}400$ m. It means that the movement was more intensive in the first case, although the slip surface was relatively shallow there. The most active zone of the landslide lies in the S–SW corner.

If the shapes and SSI magnitudes of these sections were compared, the three-dimensional character of the landslide would become clear, and in consequence, the advantage of 3D approach would be obvious.

The simulation process started from the present shape, and the figures show the final, equilibrium state in which no fur-

ther displacement occurred. However, it could not be verified if the landslide development and the final shape would agree with the simulation results. It seems that despite this disadvantage, the results give approximate information on the future landslide development. It is possible, therefore, to determine the future deformational capability of the landslide. It means, how much time and how long distance is required until the landslide reaches its equilibrium state. Difference between the present and final positions could be named “landslide potential”. The explanation of this quantity is shown on Figure 6.

The potential energy of a body depends on the height (H). The landslide in the initiation stage (1) has the greatest potential energy, i.e. landslide potential. Its movement causes decreasing the height (i.e. landslide potential). Moving landslide in the intermediate position (2) loses energy. Finally, this potential energy vanishes and the body becomes stable (3).

Simulation results show that the present landslide potential of analysed slope allows for further movement, until the horizontal displacement in X direction will be equal of about 30–35 m. Indeed, this value is approximate but can be considered as general information on the phenomenon of the landslide “energetic maturity”.

FINAL REMARKS

The investigated landslide represents mature phenomenon but not yet stabilised. The process is complex and displacements occur not only in plane X–Z but also perpendicularly to the general slope inclination. Moreover, deformational activity in different zones and the slip surface depth are differentiated. Analysis of a landslide development in some selected sections (e.g. representing the greatest inclination), only, and reduction of the problem to the two dimensions, is too big simplification. Thus, the simulation described here confirms the advantages of the 3D approach.

The simulation allowed for determining the landslide shape, the slip surface depth, and the deformational activity. The important information was obtained regarding the future behaviour of the slope, and in direct way — the “energetic maturity” of

the landslide. It was also determined that the slope equilibrium would be reached when the horizontal displacement would be equal to about 30–35 m.

However, in many cases disadvantage of the 3D modelling resulted from the poor input data, which were necessary for the construction of the spatial numerical model. Nevertheless, application of this approach may be recommended.

This research was done in frames of 5PR EC project ALARM (Assessment of Landslide Risk and Mitigation in Mountain Areas), and a scientific project “Investigation of the representative landslide process in Carpathian flysch — experimental landslide in Beskid Niski Mts.”, financially supported by the Committee of Scientific Research

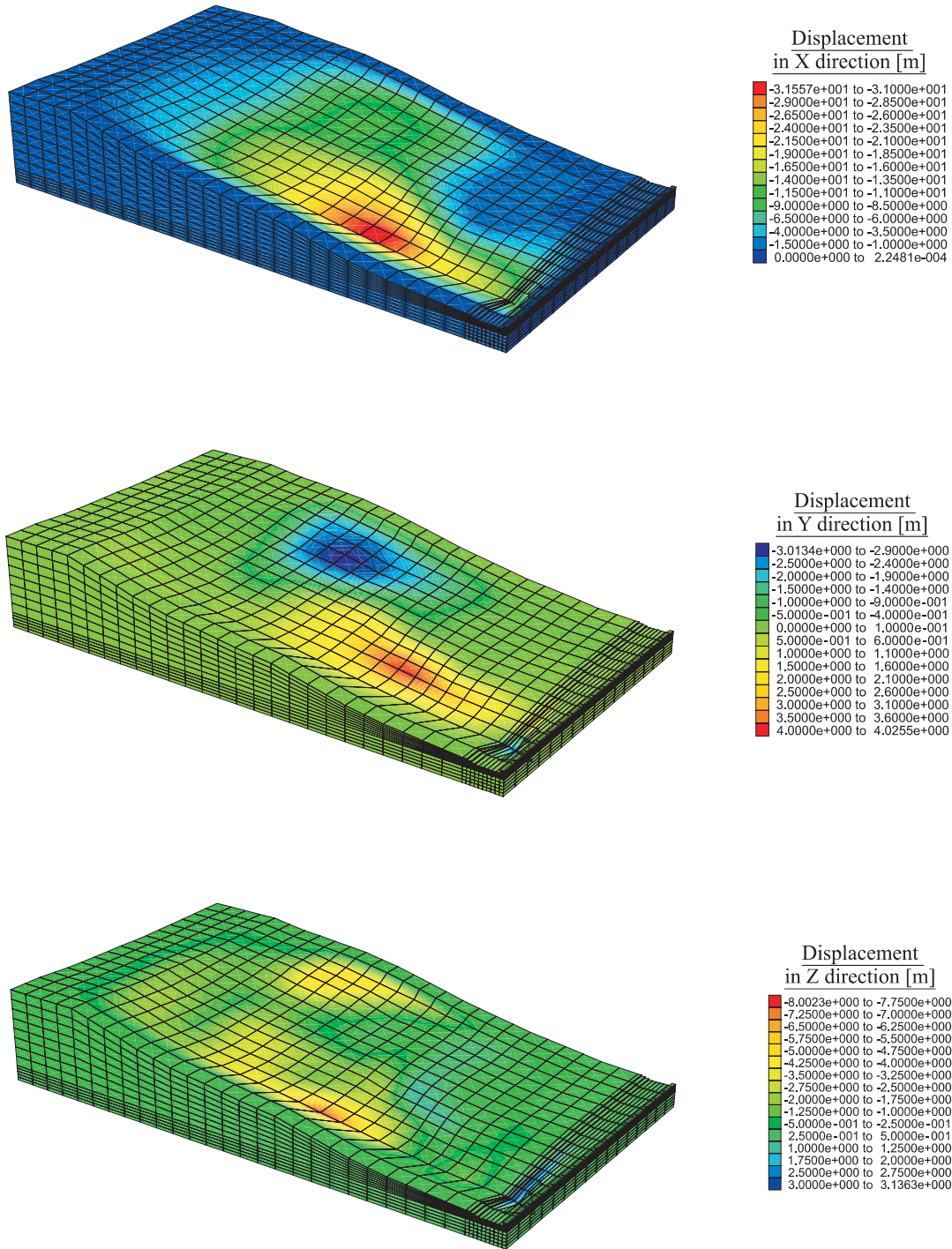


Fig. 4. Fields of displacement components in equilibrium state

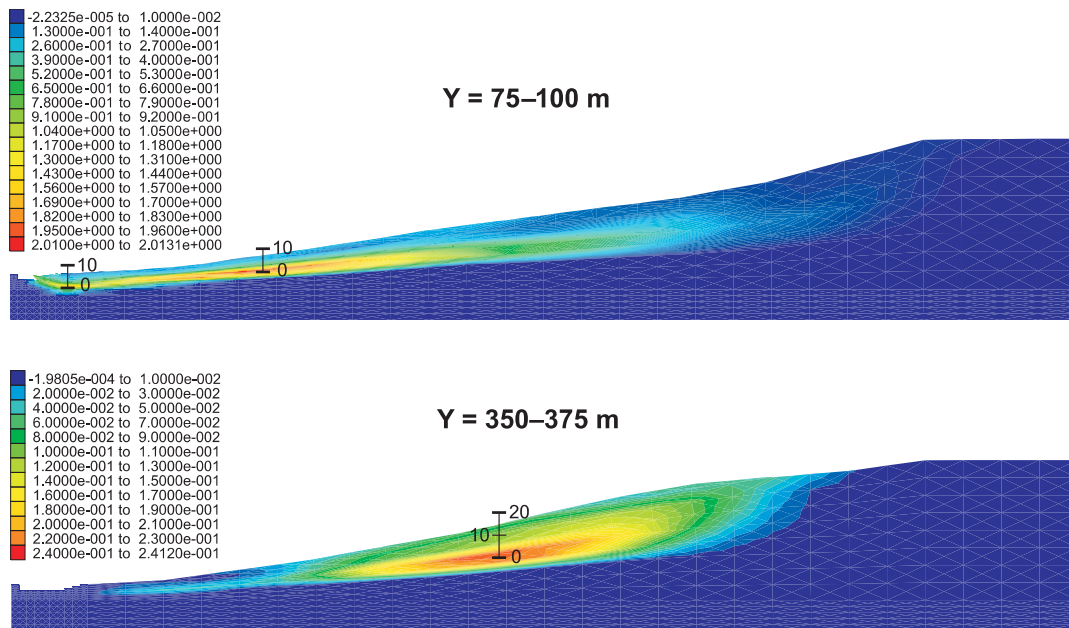


Fig. 5. Shear strain increments in different sections of the landslide

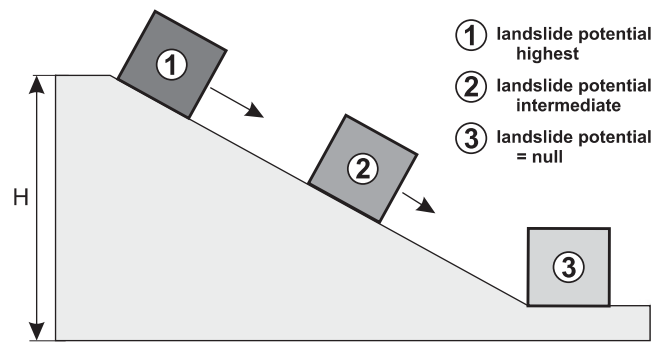


Fig. 6. Explanation of the “landslide potential” term

REFERENCES

- ITASCA C.G., 1997 — FLAC3D user's manual. Minneapolis.
- DAUKSZA L., KOTARBA A., 1973 — An analysis of the influence of fluvial erosion in the development of landslide slope. *Stud. Geomorph. Carpatho-Balcan.*, 7: 91–104.
- ZABUSKI L., GIL E., RĄCZKOWSKI W., WÓJCIK A., 2004 — Investigation of the representative landslide process in Carpathian flysch — experimental landslide in Beskid Niski Mts. Scientific Project of the Committee of Scientific Research No. 8 T12B 047 20.